sciendo

ISSN 1335-8871

MEASUREMENT SCIENCE REVIEW

Journal homepage: https://content.sciendo.com

Optimization of Component Assembly in Automotive Industry

Jaromír Křepelka[1], Petr Schovánek[1], Pavel Tuček[2,3*], Miroslav Hrabovský[1], František Jáně[3]

[1]*Joint Laboratory of Optics of Palacký University and Institute of Physics of the Czech Academy of Science, Faculty of Science, Palacký University in Olomouc, 17. listopadu 12, 771 46 Olomouc, Czech Republic*
[2]*Department of Mathematics and Physics, Faculty of Electrical Engineering and Informatics, University Pardubice, Studentská 95, 532 10 Pardubice, Czech Republic*
[3]*Hella Autotechnik Nova, Družstevní 338/16, 789 95 Mohelnice, Czech Republic, pavel.tucek@forvia.com*

Abstract: This article is devoted to the positioning of glued parts by robots in the process of manufacturing automotive headlights, with the possibility of generalization to the mutual positioning of any 3D object. The authors focused on the description of the mathematical method that leads to the optimization of the robot arm setting and ensures the closest contact of the glued parts. The contact surfaces of the two joined parts are, in the ideal case, identical in shape and their optimal alignment is considered to best align the position of the nominal points on the base part with the position of the control (measured) points on the part manipulated by the robot.

Keywords: Industry 4.0, precise positioning, automated manipulation, automotive assembly process.

1. Introduction

Modern assembly requires the use of industrial robots, which increases the efficiency of the production process, but brings problems that do not appear during conventional manual assembly. In order to meet the production quality requirements when assembling parts of automotive headlights on the assembly line, the glued headlight parts must be positioned with appropriate precision, among other things. The robot is currently a highly sophisticated device that can position the parts with sufficient accuracy, but only if its operation is programmed satisfactorily to exploit its production potential.

The example presented in this article deals with the positioning of the front headlight cover lens relative to its housing. The basic prerequisite for cover lens positioning is knowledge of the exact position of the contact surface of the headlight housing at the time of the gluing operation on the assembly line. The contact surface is located at the bottom of the groove for gluing on the cover lens. Its position is determined by the position of the nominal points in the production documentation. The coordinates of the nominal points are determined in the Cartesian coordinate system. The contact surface of the cover lens is brought into its optimum position by the robot so that the resulting position of the control points of the contact surface of the cover lens are as close as possible to the position of the nominal points in the groove of the headlight housing.

The final position of the cover lens in which the coupled part is stabilized is found by means of the rotation and displacement operations (or vice versa) [1]. The final position of this part is calculated based on the permissible position error of the relevant nominal and control points, the value of these deviations being defined in the drawing documentation. Mathematically, the final position of these points is specified by a linear combination of two objective functions denoted by $\tilde{y}_1$ and $\tilde{y}_2$. The function $\tilde{y}_1$ is defined as the sum of the squared deviations of the position of the control points from the nominal points, and the function $\tilde{y}_2$ is defined as the sum of the squared deviations from the root mean square deviation. The resulting position of the glued glass shield is given by the numerically calculated local minimum [2] of the objective function of the six variables. It also depends on the weight assigned to the partial objective functions. This weight is controlled by the designer's requirement for the tolerance of the position deviation between the control and nominal points.

2. Subject and Methods

A transformation in 3D space is required to grasp the studied problem. This transformation is a linear function determined by a rotation matrix that can be parameterized by three angles. Euler angles are often used for the transformation of two three-dimensional coordinate systems [3], [4]. An alternative is the use of three mutually orthogonal angles-yaw, pitch and roll, which is very common in robotics [5]–[8]. These two variants of rotation differ in the definition of three mutually orthogonal rotational angles that have different relationships to the original coordinate axes of the reference coordinate system, which are given by the direction of the x, y, and z axes. The usual method for determining these angles is based on quartions [8]. Other algorithms are described in [3]. A method based on a regression model with constraints is presented in [5].

DOI: 10.2478/msr-2024-0005

*Corresponding author: pavel.tucek@forvia.com (P. Tuček)

A. Rotation matrix

Euler's transformation is considered. The rotation matrices $\mathbf{R}_x$, $\mathbf{R}_y$, $\mathbf{R}_z$ around the Cartesian axes x, y, z with the angles α (a), β (b), γ (g) in the left-hand direction can be expressed with the abbreviation $c_q = \cos(q)$, $s_q = \sin(q)$, $q = a,\ b,\ g$ as

$$\mathbf{R}_x = \begin{pmatrix} 1 & 0 & 0 \\ 0 & c_a & s_a \\ 0 & -s_a & c_a \end{pmatrix},\ \mathbf{R}_y = \begin{pmatrix} c_b & 0 & -s_b \\ 0 & 1 & 0 \\ s_b & 0 & c_b \end{pmatrix},$$
$$\mathbf{R}_z = \begin{pmatrix} c_g & s_g & 0 \\ -s_g & c_g & 0 \\ 0 & 0 & 1 \end{pmatrix}. \quad (1)$$

For the right-handed rotation it is necessary to replace $s_q \to -s_q$ in (1), since sin is an odd function. The combined left-handed rotation matrix in the order x, y, z of the axes is then

$$\begin{aligned} \mathbf{R}_1 &= \mathbf{R}_z\mathbf{R}_y\mathbf{R}_x \\ &= \begin{pmatrix} c_bc_g & c_as_g + s_as_bc_g & s_as_g - c_as_bc_g \\ -c_bs_g & c_ac_g - s_as_bs_g & s_ac_g + c_as_bs_g \\ s_b & -s_ac_b & c_ac_b \end{pmatrix}. \quad (2) \end{aligned}$$

while for the z, y, x order of axes it is

$$\begin{aligned} \mathbf{R}_2 &= \mathbf{R}_x\mathbf{R}_y\mathbf{R}_z \\ &= \begin{pmatrix} c_bc_g & c_bs_g & -s_b \\ s_as_bc_g - c_as_g & c_ac_g + s_as_bs_g & s_ac_b \\ s_as_g + c_as_bc_g & c_as_bs_g - s_ac_g & c_ac_b \end{pmatrix}. \quad (3) \end{aligned}$$

The normalized rotation axis $\boldsymbol{u}$ of the rotation matrix $\mathbf{R}$ is determined by the condition $\mathbf{R}\boldsymbol{u} = \boldsymbol{u}$, which means that $\boldsymbol{u}$ is a normalized eigenvector of $\mathbf{R}$ with unit eigenvalue. If $\mathbf{R}$ has the elements $R_{i,j}$, $i,\ j = 1, 2, 3$ (or x, y, z), the rotation axis $\boldsymbol{u}$ can be obtained from the following relations

$$\boldsymbol{u}_0 = \begin{pmatrix} R_{3,2} - R_{2,3} \\ R_{1,3} - R_{3,1} \\ R_{2,1} - R_{1,2} \end{pmatrix},\ \boldsymbol{u} = \frac{\boldsymbol{u}_0}{\|\boldsymbol{u}_0\|}, \quad (4)$$

where $\|\boldsymbol{u}_0\|$ is a norm of the vector $\boldsymbol{u}_0$.

The rotation angle φ around the axis $\boldsymbol{u}$ can be calculated, for example, from the condition $2\sin\varphi = \|\boldsymbol{u}_0\|$ or from the rotation of the arbitrary non-zero vector. The rotation matrix, expressed by the rotation axis and the right-handed rotation, is as follows ($c_\varphi = \cos\varphi$, $s_\varphi = \sin\varphi$, $c = 1 - \cos\varphi$)

$$\mathbf{R} = \begin{pmatrix} c_\varphi + u_x^2c & u_xu_yc - u_zs_\varphi & u_xu_zc + u_ys_\varphi \\ u_yu_xc + u_zs_\varphi & c_\varphi + u_y^2c & u_yu_zc - u_xs_\varphi \\ u_zu_xc - u_ys_\varphi & u_zu_yc + u_xs_\varphi & c_\varphi + u_z^2c \end{pmatrix}. \quad (5)$$

Let the set of nominal points (vectors) of the investigated object be described by $\boldsymbol{R}_{0,j}$ and the corresponding measured points by $\boldsymbol{R}_{\mathrm{m},j}$, for both $j = 1, \ldots N$. Let the angles of the left-hand rotation around the axes (in the order x, y, z) be α, β, γ. The corresponding rotation matrix $\mathbf{R}$ is either $\mathbf{R}_1$ (for the rotation in the axes order x, y, z) or $\mathbf{R}_2$ (for the rotation in the axes order z, y, x).

B. Translation succeeded by rotation

Let us assume that the measured points can be translated by the vector $\boldsymbol{P}_0$ and then rotated with the matrix $\mathbf{R}$ so that the positions of the measured points are as close as possible to the corresponding nominal points. The deviations of the translated and rotated measured points from the nominal ones are as follows

$$\Delta\boldsymbol{R}_j = \mathbf{R}(\boldsymbol{R}_{\mathrm{m},j} + \boldsymbol{P}_0) - \boldsymbol{R}_{0,j}. \quad (6)$$

The objective function of an optimization problem can be defined as the sum of the squared deviation norms

$$y_1 = \frac{1}{N}\sum_{j=1}^{N} \nu_j \|\Delta\boldsymbol{R}_j\|^2, \quad (7)$$

where ν_j is the weight defined for the j-th point. These are non-negative numbers that allow us to emphasize or suppress the importance of the selected points. The aim of the task is to find six unknown quantities – three coordinates of the translation vector and three angles of the rotation matrix around the coordinate axes (or two coordinates of the normalized vector of the rotation axis and one rotation angle) – by minimizing the objective function.

Since the numerical gradient optimization method converges poorly in the default coordinate system, especially with respect to the translation vector, it is advantageous to reformulate the problem in a coordinate system where the origin is shifted to the center of gravity and to scale the problem using factor M. Finally, we seek the minimum of an objective function of six variables of the form

$$\tilde{y}_1 = \frac{1}{N}\sum_{j=1}^{N} \nu_j \|\Delta\tilde{\boldsymbol{R}}_j\|^2,\ \Delta\tilde{\boldsymbol{R}}_j = \tilde{\mathbf{R}}(\tilde{\boldsymbol{R}}_{\mathrm{m},j} + \tilde{\boldsymbol{P}}_0) - \tilde{\boldsymbol{R}}_{0,j} \quad (8)$$

where

$$\begin{aligned} &\boldsymbol{T} = \frac{1}{N}\sum_{j=1}^{N} \boldsymbol{R}_{0,j},\ \tilde{\boldsymbol{P}}_0 = M(\boldsymbol{P}_0 - \boldsymbol{T}), \\ &\tilde{\boldsymbol{R}}_{0,j} = M(\boldsymbol{R}_{0,j} - \boldsymbol{T}),\ \tilde{\boldsymbol{R}}_{\mathrm{m},j} = M(\boldsymbol{R}_{\mathrm{m},j} - \boldsymbol{T}). \quad (9) \end{aligned}$$

$\boldsymbol{T}$ is the center of gravity of the nominal points in the default coordinate system. The scaling factor M is usually chosen as a small multiple (from 1 to 10) of the reciprocal of the maximum distance of the nominal points from the center of gravity.

However, the definition of the objective function can be extended by combining the requirement for the minimum sum of squared position deviations with the requirement for the minimum sum of squared deviations from the root mean square deviation in more detail

$$\tilde{y}_2 = \frac{1}{N}\sum_{j=1}^{N} \nu_j (\|\Delta\tilde{\boldsymbol{R}}_j\| - \Delta\tilde{R}_{\mathrm{aver}})^2 \quad (10)$$

where

$$\Delta\tilde{R}_{\text{aver}} = \frac{1}{N}\left(\sum_{j=1}^{N}\|\Delta\tilde{\mathbf{R}}_j\|^2\right)^{\frac{1}{2}}. \tag{11}$$

The resulting objective function of the problem is then generally a linear combination of these two partial objective functions

$$\tilde{y} = \nu_{0,1}\tilde{y}_1 + \nu_{0,2}\tilde{y}_2 \tag{12}$$

where the numerical weights $\nu_{0,1}$ and $\nu_{0,2}$ are non-negative numbers (e.g., between 0 and 1, where their sum equals one) that determine the type of the prevailing objective function. By finding the local (ideally global) minimum of the objective function, we can assume that the problem is solved.

Finally, we obtain a solution for the original task in which the rotation matrix does not change ($\mathbf{R} = \tilde{\mathbf{R}}$) and the translation vector is

$$\boldsymbol{P}_0 = \frac{1}{M}\tilde{\boldsymbol{P}}_0 - \boldsymbol{T} + \mathbf{R}^{-1}\boldsymbol{T}. \tag{13}$$

The corrected positions of the measured points are

$$\boldsymbol{R}_{\text{cor},j} = \mathbf{R}(\boldsymbol{R}_{\text{m},j} + \boldsymbol{P}_0) \tag{14}$$

for $j = 1, \ldots N$.

C. *Rotation succeeded by translation*

The Method for solving this problem is similar to the previous case. Again, we assume that the measured points can be rotated using the rotation matrix $\mathbf{R}$ and subsequently translated by the vector $\boldsymbol{P}_0$ so that the positions of the measured points are as close as possible to the nominal points. The objective function of the problem is therefore defined analogously to the original coordinate system

$$y_1 = \frac{1}{N}\sum_{j=1}^{N}\nu_j\|\Delta\boldsymbol{R}_j\|^2,\ \Delta\boldsymbol{R}_j = \mathbf{R}\boldsymbol{R}_{\text{m},j} + \boldsymbol{P}_0 - \boldsymbol{R}_{0,j}. \tag{15}$$

In the coordinate system of the center of gravity and using the scaling factor M, it is necessary to find a minimum of the function of six variables according to (8), but using $\Delta\boldsymbol{R}_j$, which is defined in (15). The following computations rely again on the relations (8)–(12).

Finally, the problem has a solution in the default coordinate system if the rotation matrix does not change ($\mathbf{R} = \tilde{\mathbf{R}}$) and the translation vector is

$$\boldsymbol{P}_0 = \frac{1}{M}\tilde{\boldsymbol{P}}_0 - \mathbf{R}\boldsymbol{T} + \boldsymbol{T} \tag{16}$$

and the corrected parameters can be calculated according to the following relation

$$\boldsymbol{R}_{\text{cor},j} = \boldsymbol{R}\mathbf{R}_{\text{m},j} + \boldsymbol{P}_0 \tag{17}$$

for $j = 1 \ldots, N$.

3. Case Study: Numerical Application

To verify the proposed method, we construct 50 artificial nominal points lying on an elliptical curve in 3D with semi-axes of 1500 mm and 300 mm length. The "measured" points are simulated by rotating the nominal points by an angle of $(8, 5, 15)$ degrees to the left (around the axes x, y, z in this order) and then translating them by a vector of $(10, 15, 20)$ mm. When looking for the reconstruction, we must take into account the fact that the inverse solution consists of a translation followed by a rotation, but the rotation must be applied in the reverse axis order z, y, x. The result of the numerical method yields values of $(-7.999, -5, -15)$ degrees for the rotation angles $\alpha, \beta\ \gamma$ and $(-10, -15, -20)$ mm for the translation vector, numbers that are almost as expected. The average quadratic deviation of the corrected points from the nominal ones is close to zero (0.40576 μm).

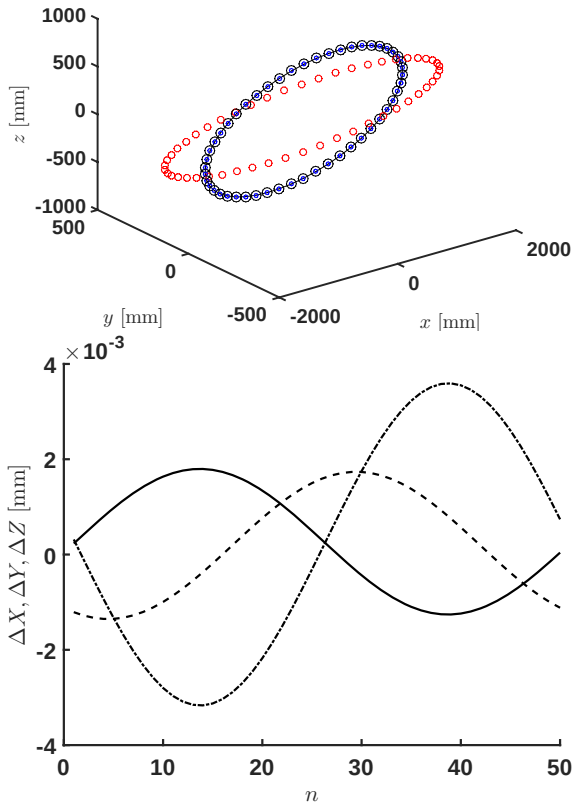

Fig. 1. (a) Positions of the points. Black circles represent nominal points, red circles are measured points and (smaller) blue circles inside the black circles are corrected points after translation and rotation (in this order). (b) Deviations of the corrected points from the nominal points: solid line for x axis, dashed line for y axis, dash-and-dot line for z axis.

Fig. 1(a) shows a 3D representation of the nominal, measured, and corrected points in the simulated case. Fig. 1(b) shows very small deviations of the corrected points from the nominal points for each Cartesian coordinate and summarizes the result of the numerical computation for the rotated and subsequently translated ellipse with simulated Gaussian-distributed measurement error, translation vector $(x, y, z) = (-9.976, -15.018, -20.139)$ mm, rotation angles $(\alpha, \beta, \gamma) = (-7.97, -5.006, -14.976)$ deg, target function $= 0.00011898$ mm^2, and root mean square deviation $= 0.24686$ mm.

Fig. 2(a) shows the 3D representation of the nominal, measured and corrected points in the case with simulated Gaussian-distributed error and a standard deviation of 1 mm. Fig. 2(b) shows the deviations of the corrected points from the nominal points for each Cartesian coordinate and for a simulated measurement error with a Gaussian distribution with a standard deviation of 1 mm.

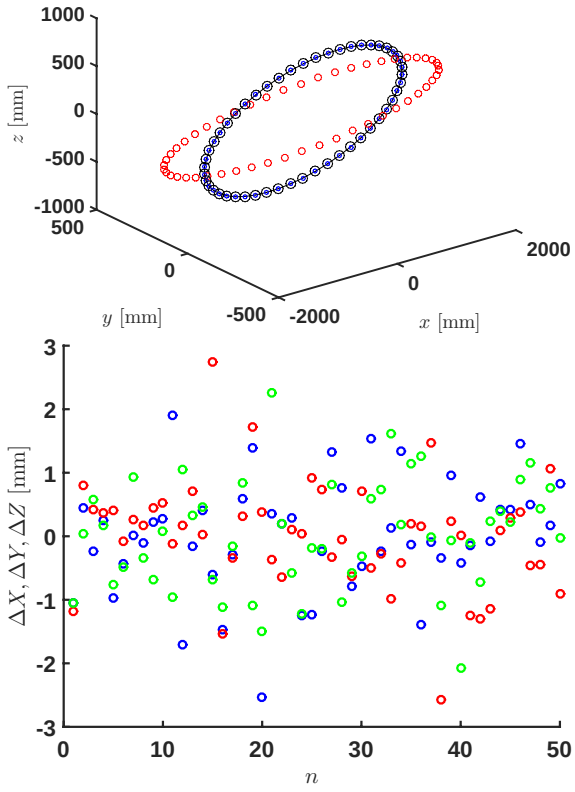

Fig. 2. (a) Positions of the points. Black circles represent nominal points, red circles are measured points, and (smaller) blue circles inside the black circles are corrected points after translation and rotation (in that order). (b) Deviations of the corrected points from the nominal points and for the simulated measurement error with a Gaussian distribution with a standard deviation of 1 mm: blue circles for the x axis, red circles for the y axis, green circles for the z axis.

In the third example, actual data from a practical measurement of the cover lens alignment for 22 points are processed. Due to the very small differences between the nominal and measured points, the figures of the type analogously to Fig. 1(a), and Fig. 2(a) are not illustrative. However, we can distinguish two possible solutions to the glass alignment problem. For the first one we have the result where we use a translation vector of $(0.039, -1.022, -1.145)$ mm and a subsequent rotation around the x, y, z axes with angles of $(0.016, 0.018, -0.014)$ degrees (or equivalently around the rotation axis of $(-0.578, -0.635, 0.512)$ mm with a rotation angle of 0.0283 degrees). We conclude that the root mean square deviation of 0.12237 mm for the corrected points is smaller than the value of 0.16319 mm that applies to the measured points.

In Fig. 3 we see the norms $\Delta\boldsymbol{R}$ of the deviation vectors (calculated from their x, y, z components) for 22 measured points, which are mostly closer to zero.

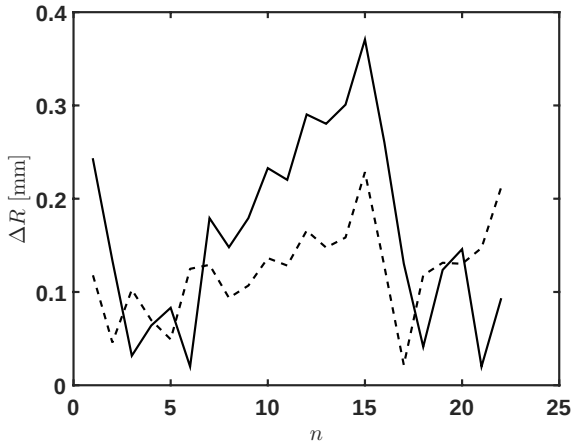

Fig. 3. Normalized values of the deviations of the measured points from the nominal points (solid line) and for the corrected points (dashed line) for the practical example and for the translation followed by the rotation.

The second case (which can also be obtained from the first case by applying the direct transformation described in section 3) consists of applying a rotation followed by a translation. The parameters of this procedure are the rotation angle of $(0.016, 0.018, -0.014)$ deg and the translation vector of $(0.04, -1.022, -1.145)$ mm, which are almost the same values as in the previous case due to the very small values of the rotation angles and the components of the translation vector. The average corrected deviations are also the same, which is why we do not repeat the corresponding table and figure.

4. Discussion

1) For both cases mentioned above, the mean values of the deviations and root mean square deviations for measured and corrected quantities can be determined using the formulae

$$\begin{aligned}
\Delta R_0 &= \frac{1}{N}\sum_{j=1}^{N} \|\boldsymbol{R}_{\mathrm{m},j} - \boldsymbol{R}_{0,j}\|, \\
\Delta R_{0,2} &= \frac{1}{N}\sum_{j=1}^{N} \|\boldsymbol{R}_{\mathrm{m},j} - \boldsymbol{R}_{0,j}\|^2, \\
\Delta R_{\mathrm{cor}} &= \frac{1}{N}\sum_{j=1}^{N} \|\boldsymbol{R}_{\mathrm{cor},j} - \boldsymbol{R}_{0,j}\|, \\
\Delta R_{\mathrm{cor},2} &= \frac{1}{N}\sum_{j=1}^{N} \|\boldsymbol{R}_{\mathrm{cor},j} - \boldsymbol{R}_{0,j}\|^2. \qquad (18)
\end{aligned}$$

This result in the variances of the deviations

$$\sigma_0 = \sqrt{\Delta R_{0,2} - (\Delta R_0)^2},\ \sigma_{\mathrm{cor}} = \sqrt{\Delta R_{\mathrm{cor},2} - (\Delta R_{\mathrm{cor}})^2} \qquad (19)$$

which serve as qualitative criteria for the optimization process.

2) In particular, the translations along the grooves are not important for the alignment of the cover lens, which is the reason for improving the objective functions and calculating

only the projections of these vector deviations onto a plane perpendicular to the tangent of the groove line, rather than the deviations of the corrected positions from the nominal positions. For this purpose, we can, for example, introduce the unit vectors defining the tangent directions of the groove for the j-th nominal point as $\boldsymbol{d}_j$. Then, we can construct again the objective function $\tilde{y} = v_{0,1}\tilde{y}_1 + v_{0,2}\tilde{y}_2$ in the translated and scaled coordinate system using the objective functions, but with a substitution

$$\begin{aligned} \tilde{y}_1 &= \frac{1}{N}\sum_{j=1}^{N} v_j \left(\Delta\tilde{\boldsymbol{R}}_j\right)^2, \\ \tilde{y}_2 &= \frac{1}{N}\sum_{j=1}^{N} v_j \left(|\Delta\tilde{\boldsymbol{R}}_j \cdot \boldsymbol{d}_j| - \Delta\tilde{R}_{\text{aver}}\right)^2 \end{aligned} \tag{20}$$

where only the projections of the deviation vectors are applied.

5. Case study – practical application

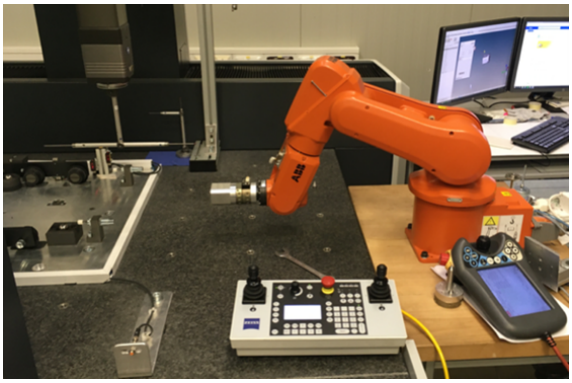

Fig. 4. Starting position, the robot is holding a part in a predefined position, which is scanned and the trajectory is calculated.

Precise positioning is an essential aspect of assembly processes that require accurate alignment of parts and components. The ability to position parts with high accuracy is crucial in industries such as electronics, aerospace and automotive manufacturing, where even minor misalignments can cause significant problems. Precise positioning is achieved through the use of advanced technologies such as robotics, computer vision and precision sensors. Regardless of which method is used, there are always other that affect the final alignment, such as the mechanical behavior of robots. In visual positioning, cameras and computer vision algorithms are used to detect and analyze the position and orientation of the parts. Force control uses sensors and feedback mechanisms to control the forces applied during the assembly process, and ensure that the parts are aligned and attached with the correct force. Feedback control uses sensors to monitor the position and movement of parts during assembly and provide feedback to the positioning system to adjust and correct any misalignment.

Robotic systems play a significant role in precise positioning in assembly processes. Robotic arms can be programmed to perform precise movements, enabling accurate positioning of parts. In addition, robots can be equipped with sensors and computer vision systems that allow them to detect and analyze the position and orientation of parts during assembly. Nevertheless, precise positioning is a critical aspect of assembly processes that require achieving a precise position within a certain cycle time. By using the above technique, manufacturers can ensure that their products are assembled with high accuracy, reducing the risk of defects and improving product quality. A practical application of the above-designed algorithm was carried out on an original component taken from a random position. The goal of the practical case study was to implement the methodology in a real environment, where we also took into account the random positioning errors caused by the robot itself. The case study followed the standard assembly steps (see the results in Table 1, Table 2, Table 3 and Fig. 4, Fig. 5)

- *the object is removed from the box,*
- *measuring of the starting position,*
- *setting the final position,*
- *measuring of the final position,*
- *correction until the final position with predefined tolerances is reached.*

Table 1. Measured coordinates X, Y, Z of 12 points on a surface, position 1.

Points	X[mm]	Y[mm]	Z[mm]
A1	591.525	6.835	172.543
A2	561.655	9.466	173.451
A3	589.818	−13.040	173.977
A4	559.948	−10.410	174.885
B1	591.533	19.333	136.573
B2	561.662	21.964	137.481
B3	592.260	20.709	156.513
B4	562.389	23.340	157.421
C1	597.894	−21.639	134.154
C2	600.454	8.174	132.003
C3	598.985	−19.574	164.063
C4	601.545	10.239	161.912

Table 2. Measured coordinates X, Y, Z of 12 points in the intermediate step, position 2.

Points	X[mm]	Y[mm]	Z[mm]
A1	590.530	8.726	174.296
A2	560.549	9.773	174.531
A3	589.836	−11.255	174.826
A4	559.855	−10.208	175.060
B1	590.744	22.796	138.913
B2	560.764	23.842	139.147
B3	590.919	23.319	158.905
B4	560.938	24.366	159.139
C1	599.308	−17.646	134.895
C2	600.348	12.325	134.101
C3	599.569	−16.861	164.884
C4	600.609	13.111	164.090

Table 3. Final coordinates X, Y, Z of 12 points corresponding to the target position (position 3).

Points	X[mm]	Y[mm]	Z[mm]
A1	590	10	175
A2	560	10	175
A3	590	−10	175
A4	560	−10	175
B1	590	25	140
B2	560	25	140
B3	590	25	160
B4	560	25	160
C1	600	−15	135
C2	600	15	135
C3	600	−15	165
C4	600	15	165

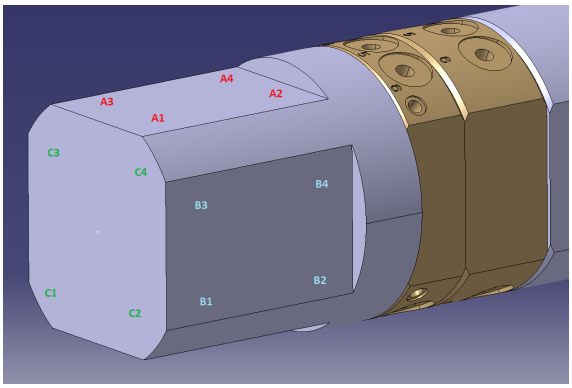

Fig. 5. Intermediate iteration of a positioning. The targeted position was not reached for various reasons (robot misalignment, positioning error, gripper, etc.).

6. Conclusion

In this paper, we have advocated the use of mathematical modeling for problems in the automotive industry. Our approach represents our pilot contribution to intractable problems in the automation of headlight manufacturing process. Our future objective is to design a multipurpose tool to compare objects, search for objects and test hypotheses about their geometric shape. The main idea to identify the headlight is based on the determination of the Euler transformation matrix. The most important features are the robustness of the methodology and the knowledge of the metrological uncertainties of the estimates. The performed numerical study proved that the accuracy of the estimate is sufficient to use our model in practice. Finally, the proposed methodology was tested on a real application for the precise manipulation and positioning of original equipment positioned by the robot. The practical example proved the reliability of the method.

Acknowledgement

This contribution has been supported by the institutional support of HELLA. The authors are also grateful to the Palacký University in Olomouc, Czech Republic, and the University of Pardubice, Czech Republic for knowledge sharing and long-term cooperation in the field of mathematical and computer modeling. The authors thanks also for the support of the project funded by the Ministry of Education, Youth and Sports of the Czech Republic (project CZ.02.1.01/0.0/0.0/17_049/0008422). We also thank all colleagues at Hella Autotechnik Nova (namely Oldřich Mišurec, Petr Sysel, and Tomáš Mazurka) for their help with the practical application.

References

[1] Howard, A. (1987). *Elementary Linear Algebra*. Wiley, ISBN 0-471-84819-0.

[2] Press, W. H., Teukolsky, S. A., Vetterling, W. T., Flannery, B. P. (1992). *Numerical Recipes in Fortran 77: The Art of Scientific Computing (2nd Ed.)*. Cambridge University Press, ISBN 0-521-43064-X.

[3] Janota, A., Šimák, V., Nemec, D., Hrbček, J. (2015). Improving the precision and speed of Euler angles computation from low-cost rotation sensor data. *Sensors*, 15(3), 7016–7039. https://doi.org/10.3390/s150307016

[4] Shuster, M. D., Markley, F. L. (2006). General formula for extracting the Euler angles. *Journal of Guidance, Control and Dynamics*, 29(1), 215. https://doi.org/10.2514/1.16622

[5] Svoboda, M., Marek, J., Heckenbergerová, J. (2014). Estimation of angles yaw, pitch and roll in a special transformation problem. In *Nostradamus 2014: Prediction, Modeling and Analysis of Complex Systems*. Springer, AISC 289, 393–400. https://doi.org/10.1007/978-3-319-07401-6_39

[6] Sun, Z., Dadalau, A., Verl, A. (2014). Generation of rotation matrix for assembly models with arbitrary angle constraints. *The International Journal of Advanced Manufacturing Technology*, 74, 563–568. https://doi.org/10.1007/s00170-014-5907-3

[7] Timmermans, S., Leys, F., Vandepitte, D. (2017). Model-based evaluation of control roll, pitch, yaw moments for a robotic hummingbird. *Journal of Guidance, Control and Dynamics*, 40 (11), 2933–2939. https://doi.org/10.2514/1.G002819

[8] Zhang, X., Xia, B., Tao, T., Zhang, M. (2016). The design of the attitude detection algorithm of underwater robot. In *2016 Sixth International Conference on Instrumentation & Measurement, Computer, Communication and Control (IMCCC)*, IEEE, 984–988. https://doi.org/10.1109/IMCCC.2016.165

Received April 21, 2023
Accepted January 08, 2024